Inorg. Chem. **2007**, *46*, 4239–4247

Square-Planar $N_2S_2Ni^{II}$ Complexes with an Extended π-Conjugated System

Tatsuya Kawamoto,* Kazunori Takeda, Masato Nishiwaki, Takashi Aridomi, and Takumi Konno

Department of Chemistry, Graduate School of Science, Osaka University, 1-16 Machikaneyama, Toyonaka, Osaka 560-0043, Japan

Received September 25, 2006

The reaction of a mixture of 2-(1-naphthyl)benzothiazoline (HL^1) and 2,6-diphenylbenzo[1,2-*d*:4,5-*d*′]bisthiazoline (H_3L^2) with nickel(II) acetate tetrahydrate yielded three kinds of square-planar nickel(II) complexes: one nickel(II) complex with innocent ligands ($[Ni(L^1)_2]$ (**1c**)) and two nickel(II) complexes with non-innocent ligands ($[Ni(L^1–L^1)]$ (**1a**) and $[Ni(L^1–L^2)]$ (**1b**)). The complex **1c** has two bidentate-N,S ligands, which are formed via ring opening of HL^1. On the other hand, the two complexes **1a** and **1b** contain a tetradentate-N_2S_2 ligand, which is created via ring opening of HL^1 and H_3L^2, followed by bond formation between imino carbon atoms. Complexes **1a** and **1b** show very intense absorptions in the near-infrared (NIR) region, characteristic of square-planar complexes with non-innocent ligands. The third nickel(II) complex having a non-innocent tetradentate-N_2S_2 ligand ($[Ni(L^2–L^2)]$ (**2**)) was prepared from H_3L^2 and nickel(II) acetate tetrahydrate. The electronic spectrum of **2** exhibits a very intense absorption at 981 nm ($\epsilon = 3.6 \times 10^4$ M^{-1} cm^{-1}), which is significantly red-shifted compared with those of **1a** (837 nm and 4.4×10^4 M^{-1} cm^{-1}) and **1b** (885 nm and 4.5×10^4 M^{-1} cm^{-1}), indicating the presence of an extended π delocalization. The reaction of 2,6-bis(3,5-dichlorophenyl)benzo[1,2-*d*:4,5-*d*′]bisthiazoline (H_3L^3) with nickel(II) acetate tetrahydrate also led to the formation of a nickel(II) complex with a non-innocent ligand ($[Ni(L^3–L^3)]$ (**3**)). While complex **3** is analogous to **2**, its electrical conductivity is much higher than that of **2**. The molecular structures of **1b**, **1c**, **2**, and **3** were determined by X-ray crystallography.

Introduction

Since the early 1960s, transition-metal complexes displaying non-innocent redox behavior, typified by dithiolene metal complexes, have received much attention[1] because of their attractive properties such as conductivity and magnetism.[2] In particular, considerable research efforts have been centered on the development of single-component molecular conductors,[3,4] prompted by the discovery of the dithiolene complex $[Ni(tmdt)_2]$ (tmdt = trimethylenetetrathiafulvalenedithiolate), which shows a very high conductivity.[5] In addition, metal complexes with non-innocent ligands are expected as a new family of near-infrared (NIR)-absorbing dyes because they tend to exhibit a very intense absorption in the NIR region.[6,7] Such metal complexes, therefore, possess a great possibility

* To whom correspondence should be addressed. E-mail: kaw@ch.wani.osaka-u.ac.jp.

(1) (a) McCleverty, J. A. *Prog. Inorg. Chem.* **1968**, *10*, 49. (b) Schrauzer, G. N. *Acc. Chem. Res.* **1969**, *2*, 72. (c) Holm, R. H.; O'Connor, M. J. *Prog. Inorg. Chem.* **1971**, *14*, 241. The term "non-innocent", which was introduced by Jørgensen [Jørgensen, C. K. *Struct. Bonding (Berlin)* **1966**, *1*, 234], is often used for a redox-active complex. The recent reports have suggested that non-innocent behavior in the square-planar complexes ($[M(L)_2]$) is provided by the ligands that consist of two radical monoanions having antiferromagnetically coupled spins. See ref 7. The term "innocent" is used for ligands that are not "non-innocent".

(2) Stiefel, E. I. *Prog. Inorg. Chem.* **2004**, *52*.

(3) Mitsumi, M.; Goto, H.; Umebayashi, S.; Ozawa, Y.; Kobayashi, M.; Yokoyama, T.; Tanaka, H.; Kuroda, S.; Toriumi, K. *Angew. Chem., Int. Ed.* **2005**, *44*, 4164.

(4) Llusar, R.; Uriel, S.; Vicent, C.; Clemente-Juan, J. M.; Coronado, E.; Gómez-García, C. J.; Braïda, B.; Canadell, E. *J. Am. Chem. Soc.* **2004**, *126*, 12076.

(5) Tanaka, H.; Okano, Y.; Kobayashi, H.; Suzuki, W.; Kobayashi, A. *Science* **2001**, *291*, 285.

(6) (a) Campbell, J.; Jackson, D. A.; Stark, W. M.; Watson, A. A. *Dyes Pigm.* **1991**, *15*, 15. (b) Fabian, J.; Nakazumi, H.; Matsuoka, M. *Chem. Rev.* **1992**, *92*, 1197. (c) Bigoli, F.; Cassoux, P.; Deplano, P.; Mercuri, M. L.; Pellinghelli, M. A.; Pintus, G.; Serpe, A.; Trogu, E. F. *J. Chem. Soc., Dalton Trans.* **2000**, 4639. (d) Schwab, P. F. H.; Diegoli, S.; Biancardo, M.; Bignozzi, C. A. *Inorg. Chem.* **2003**, *42*, 6613.

(7) (a) Chaudhuri, P.; Verani, C. N.; Bill, E.; Bothe, E.; Weyhermüller, T.; Wieghardt, K. *J. Am. Chem. Soc.* **2001**, *123*, 2213. (b) Herebian, D.; Bothe, E.; Bill, E.; Weyhermüller, T.; Wieghardt, K. *J. Am. Chem. Soc.* **2001**, *123*, 10012. (c) Herebian, D.; Bothe, E.; Neese, F.; Weyhermüller, T.; Wieghardt, K. *J. Am. Chem. Soc.* **2003**, *125*, 9116. (d) Min, K. S.; Weyhermüller, T.; Bothe, E.; Wieghardt, K. *Inorg. Chem.* **2004**, *43*, 2922. (e) Ray, K.; Weyhermüller, T.; Neese, F.; Wieghardt, K. *Inorg. Chem.* **2005**, *44*, 5345.

10.1021/ic0618246 CCC: $37.00
Published on Web 04/10/2007

Scheme 1

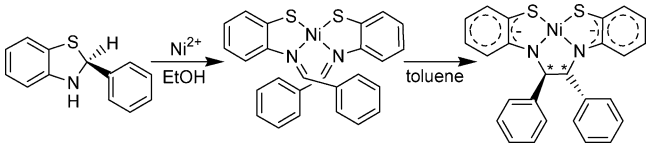

to be applied as attractive multifunctional materials. However, only a few examples of metal complexes with noninnocent ligands have been recognized to exhibit multifunctional properties,[8] except for those showing conductivity and magnetism.[9]

Previously, we found a facile synthetic method, not electrochemical oxidation or reduction, of d^8 metal complexes (M = Ni, Pt) having a unique N_2S_2 donor set that show intense absorptions in the range of 700−850 nm (Scheme 1).[10] Furthermore, based on this synthetic method, we have synthesized nickel(II) complexes with an extended π-conjugated system that show an intense absorption band at lower energy of ca. 950 nm, although their structures and electronic properties remained uncertain.[11] Herein we report on the synthesis and characterization of a family of nickel(II) complexes with an extended π-conjugated system that is regarded as a potential multifunctional material for NIR-absorbing dye and conductor.

Experimental Section

General Procedures. All of the synthetic reactions were carried out under an inert gas atmosphere using standard Schlenk techniques. Workup procedures, including column chromatography, were performed in air. The reagents were commercial samples and were not purified further. 2-(1-Naphthyl)benzothiazoline (HL^1)[12] and 2,6-diphenylbenzo[1,2-*d*:4,5-*d*′]bisthiazoline (H_3L^2)[11] were prepared as described previously. The absorption and diffuse-reflectance spectra were recorded with a Jasco V-570 spectrophotometer at room temperature. The reflectance spectra on $MgSO_4$-diluted samples were transformed into absorption spectra by using the Kubelka−Munk equation. The ^{1}H NMR spectra were recorded with a JEOL GSX 500 spectrometer. The IR spectra in the region of 4000−400 cm^{-1} were measured on a Jasco FT/IR-550 spectrometer by using Nujol mulls. Voltammetric studies were performed by a CV-600A apparatus (BAS) with complex concentrations of 0.5 mM at 25 °C in 0.1 mol dm^{-3} $[Bu_4N]BF_4/CH_2Cl_2$ with a glassy-carbon working electrode, a Ag/Ag^+ reference electrode, and a platinum-wire auxiliary electrode. The scan rates were 100 mV s^{-1}. Spectroelectrochemical studies were performed by a CV-600A apparatus (BAS) using a thin-layer quartz cell (0.5 mm light path length) with a platinum-mesh (100 mesh) working electrode. The computational details of the discrete variational (DV)−Xα method used in the present work have been described elsewhere.[13] The atomic radius R_0 for each atom was obtained from the values determined by Slater.[14] The sample points were taken up to 90 000. Self-consistency within 0.003e was obtained for the orbital populations. Electrical resistivities of complexes **2** and **3** were measured at room temperature for compacted pellets by the conventional two-probe method.[15] Elemental analyses were performed at Osaka University.

Synthesis of 2,6-Bis(3,5-dichlorophenyl)benzo[1,2-*d*:4,5-*d*′]-bisthiazoline (H_3L^3). To a solution of NaOH (0.18 g, 4.5 mmol) in 30 mL of hot ethanol was added 2,5-diamino-1,4-benzenethiol dihydrochloride (0.20 g, 0.82 mmol) and 3,5-dichlorobenzaldehyde (0.29 g, 1.6 mmol). The mixture was refluxed for 2 h and then allowed to cool to room temperature. The light-yellow powder precipitated was collected by filtration. The powder was dissolved in 200 mL of THF, and insoluble NaCl was removed by filtration. The resulting yellow solution was evaporated to dryness to afford a yellow powder. Yield: 0.25 g, 61%. Anal. Found: C, 50.33; H, 2.88; N, 5.93. Calcd for H_3L^3·0.25THF: C, 50.02; H, 2.80; N, 5.55. IR (Nujol; cm^{-1}): 3238 (ν_{N-H}). ^{1}H NMR (500 MHz, DMSO-d_6): δ 7.51 (s, 2H), 7.46 (d, 4H), 6.58 (d, 2H), 6.54 (br s, 2H), 6.32 (t, 2H).

Synthesis of [Ni(L^1−L^1)] (1a), [Ni(L^1−L^2)] (1b), and [Ni(L^1)$_2$] (1c). To a light-yellow suspension containing HL^1 (0.53 g, 2.0 mmol) and H_3L^2 (0.32 g, 0.92 mmol) in 60 mL of ethanol was added nickel(II) acetate tetrahydrate (0.55 g, 2.2 mmol). The reaction mixture was refluxed for 3 h and allowed to cool in a refrigerator overnight. The greenish-brown powder precipitated was collected by filtration and redissolved in 100 mL of CH_2Cl_2. After filtration, the greenish-brown filtrate was concentrated to ca. 20 mL and poured onto a silica gel column. The separation with CH_2Cl_2/*n*-hexane (5:1) eluent gave mainly three bands. The first purple and second green bands were collected and evaporated to dryness, yielding **1a** as a purple powder (12 mg) and **1b** as a green powder (45 mg). The green product **1b** was recrystallized from $CHCl_3$/CH_3OH in a refrigerator. The third red band was also collected and evaporated to dryness, yielding **1c** as a red-brown powder (55 mg). This red-brown product was recrystallized from CH_2Cl_2/*n*-hexane. **1a.** Anal. Found: C, 66.52; H, 5.55; N, 3.92. Calcd for **1a**·0.75CH_2Cl_2·C_6H_{14}: C, 66.75; H, 5.43; N, 3.82. IR (Nujol; cm^{-1}): 1595 and 1570 ($\nu_{C=C}$). ^{1}H NMR (500 MHz, $CDCl_3$): δ 8.30 (d, 2H), 8.00 (d, 2H), 7.79 (d, 2H), 7.71 (d, 2H), 7.64 (t, 2H), 7.54 (t, 2H), 7.32 (d, 2H), 7.20 (t, 2H), 7.15 (s, 2H), 7.07 (t, 2H), 7.01 (d, 2H), 6.81 (t, 2H). UV/vis/NIR (CH_2Cl_2): λ_{max}/nm (ϵ/M^{-1} cm^{-1}) 1143 (4.0×10^3), 985 (3.4×10^3), 837 (4.4×10^4), 353sh (6.3×10^3). **1b.** Anal. Found: C, 61.01; H, 3.72; N, 5.74. Calcd for Ni(L^1−L^2)·0.5$CHCl_3$·CH_3OH: C, 60.99; H, 3.92; N, 5.54. IR (Nujol; cm^{-1}): 1597 and 1570 ($\nu_{C=C}$). ^{1}H NMR (500 MHz, $CDCl_3$): δ 8.47 (d, 1H), 8.24 (s, 1H), 8.01−7.98 (m, 3H), 7.82 (t, 1H), 7.76 (d, 1H), 7.74 (d, 1H), 7.69 (t, 1H), 7.65 (s, 1H), 7.59 (d, 2H), 7.50

(8) (a) Smucker, B. W.; Hudson, J. M.; Omary, M. A.; Dunbar, K. R. *Inorg. Chem.* **2003**, *42*, 4714. (b) Kobayashi, A.; Sasa, M.; Suzuki, W.; Fujiwara, E.; Tanaka, H.; Tokumoto, M.; Okano, Y.; Fujiwara, H.; Kobayashi, H. *J. Am. Chem. Soc.* **2004**, *126*, 426.

(9) (a) Imai, H.; Otsuka, T.; Naito, T.; Awaga, K.; Inabe, T. *J. Am. Chem. Soc.* **1999**, *121*, 8098. (b) Aonuma, S.; Casellas, H.; Faulmann, C.; Garreau, de Bonneval, B.; Malfant, I.; Cassoux, P.; Lacroix, P. G.; Hosokawa, Y.; Inoue, K. *J. Mater. Chem.* **2001**, *11*, 337. (c) Mukai, K.; Senba, N.; Hatanaka, T.; Minakuchi, H.; Ohara, K.; Taniguchi, M.; Misaki, Y.; Hosokoshi, Y.; Inoue, K.; Azuma, N. *Inorg. Chem.* **2004**, *43*, 566.

(10) The reaction of 2-phenylbenzothiazoline with a nickel(II) ion leads to a Schiff base nickel(II) complex via deprotonation with a ring-opening reaction. Upon stirring of the toluene solution of the Schiff base complex, a nickel(II) complex with a non-innocent ligand is formed through C−C bond formation. The connected carbon atoms are asymmetric. Both of the nickel(II) complexes, which have the same chemical compositions, can be correlated to each other as valence isomers. See: (a) Kawamoto, T.; Nagasawa, I.; Kuma, H.; Kushi, Y. *Inorg. Chim. Acta* **1997**, *265*, 163. (b) Kawamoto, T.; Kuma, H.; Kushi, Y. *Bull. Chem. Soc. Jpn.* **1997**, *70*, 1599. (c) Kawamoto, T.; Kushi, Y. *Bull. Chem. Soc. Jpn.* **2004**, *77*, 289.

(11) Kawamoto, T.; Konno, T. *Mol. Cryst. Liq. Cryst.* **2002**, *379*, 443.

(12) Kawamoto, T.; Nagasawa, I.; Kuma, H.; Kushi, Y. *Inorg. Chem.* **1996**, *35*, 2427.

(13) Adachi, H.; Tsukada, M.; Satoko, C. *J. Phys. Soc. Jpn.* **1978**, *45*, 875.

(14) Slater, J. C. *Symmetry and Energy Bands in Crystals*; Dover Publications, Inc.: New York, 1972; p 55.

(15) Nakahama, A.; Nakano, M.; Matsubayashi, G. *Inorg. Chim. Acta* **1999**, *284*, 55.

Table 1. Crystallographic Data for **1b**, **1c**, **2**, and **3**

	1b	**1c**·CH_2Cl_2	**2**·$2CH_2Cl_2$	**3**·CH_2Cl_2·DMF
empirical formula	$C_{37}H_{25}N_3NiS_3$	$C_{35}H_{26}Cl_2N_2NiS_2$	$C_{42}H_{30}Cl_4N_4NiS_4$	$C_{45}H_{29}Cl_{12}N_5NiOS_4$
M	666.49	668.31	919.45	1268.08
cryst syst	monoclinic	monoclinic	triclinic	triclinic
space group	$P2_1/n$	$P2_1/n$	$P\bar{1}$	$P\bar{1}$
a/Å	11.730(8)	12.507(2)	11.375(8)	11.85(3)
b/Å	18.139(13)	13.842(3)	12.467(10)	12.63(4)
c/Å	13.679(5)	18.215(3)	15.068(11)	19.59(5)
α/deg			97.94(6)	95.0(3)
β/deg	94.60(3)	91.916(14)	109.01(5)	102.3(2)
γ/deg			93.77(6)	113.6(2)
V/Å^3	2901(3)	3151.5(10)	1987(3)	2575(12)
Z	4	4	2	2
F(000)	1376	1376	940	1276
D_{calcd}/g cm^{-3}	1.526	1.409	1.537	1.635
μ/mm^{-1}	0.919	0.945	1.006	1.204
R1[a] (obsd)	0.0579	0.0451	0.0689	0.0795
wR2[b] (all)	0.1216	0.1535	0.2114	0.2467

[a] $R1 = \sum(||F_o| - |F_c||)/\sum(|F_o|)$. [b] $wR2 = [\sum w(F_o^2 - F_c^2)^2/\sum w(F_o^2)^2]^{1/2}$.

(t, 1H), 7.44 (d, 2H), 7.38−7.31 (m, 3H), 7.18 (s, 1H), 7.15 (d, 1H), 7.12 (t, 1H), 7.02 (d, 1H), 6.91 (t, 1H), 6.85 (d, 1H), 6.32 (s, 1H). UV/vis/NIR (CH_2Cl_2): λ_{max}/nm (ϵ/M^{-1} cm^{-1}) 1229 (6.6 × 10^3), 1048 (4.5 × 10^3), 885 (4.5 × 10^4), 361 (2.0 × 10^4). **1c.** Anal. Found: C, 63.02; H, 4.04; N, 4.27. Calcd for **1c**·CH_2Cl_2: C, 62.90; H, 3.92; N, 4.19. IR (Nujol; cm^{-1}): 1593 and 1574 ($\nu_{C=N}$ and $\nu_{C=C}$). ^{1}H NMR (500 MHz, $CDCl_3$): δ 10.73 (d, 2H), 8.19 (s, 2H), 7.95 (d, 2H), 7.84 (d, 2H), 7.60 (t, 2H), 7.41 (d, 2H), 7.39 (t, 2H), 7.16 (t, 2H), 7.03 (d, 2H), 7.01 (t, 2H), 6.59 (t, 2H), 5.89 (d, 2H). UV/vis/NIR (CH_2Cl_2): λ_{max}/nm (ϵ/M^{-1} cm^{-1}) 513sh (3.3 × 10^3), 467 (3.9 × 10^3), 344 (1.3 × 10^3).

Synthesis of 1c (Direct Synthetic Method). A suspension of HL^1 (0.11 g, 0.42 mmol) and nickel(II) acetate tetrahydrate (0.06 g, 0.24 mmol) in 20 mL of ethanol was heated to reflux for 30 min. A dark-red precipitate was collected by filtration. Yield: 0.07 g, 57%.

Synthesis of [Ni(L^2−L^2)] (2). To a light-yellow suspension of H_3L^2 (0.32 g, 0.92 mmol) in 30 mL of ethanol was added nickel(II) acetate tetrahydrate (0.30 g, 1.2 mmol). The reaction mixture was refluxed for 2 h and allowed to cool in a refrigerator overnight. The resulting green powder was collected by filtration and redissolved in 50 mL of CH_2Cl_2. After filtration, the green product was dried in vacuo and recrystallized from dimethylformamide (DMF)/CH_2Cl_2. Yield: 0.07 g, 17%. Anal. Found: C, 56.59; H, 3.85; N, 7.03. Calcd for **2**·0.5DMF·1.5CH_2Cl_2: C, 56.53; H, 3.59; N, 6.90. IR (Nujol; cm^{-1}): 1601, 1584, and 1572 ($\nu_{C=N}$ and $\nu_{C=C}$). UV/vis/NIR (DMF): λ_{max}/nm (ϵ/M^{-1} cm^{-1}) 1559 (4.4 × 10^3), 981 (3.6 × 10^4), 572 (1.4 × 10^4), 514 (1.3 × 10^4), 404 (4.5 × 10^4). Electrical conductivity (S cm^{-1}): 5.9 × 10^{-8}.

Synthesis of [Ni(L^3−L^3)] (3). To a yellow suspension of H_3L^3 (0.47 g, 0.93 mmol) in 30 mL of ethanol was added nickel(II) acetate tetrahydrate (0.30 g, 1.2 mmol). The reaction mixture was refluxed for 3 h and allowed to cool in a refrigerator overnight. The resulting green powder was collected by filtration and redissolved in 50 mL of CH_2Cl_2. After filtration, the dark-green product was dried in vacuo and recrystallized from DMF/CH_2Cl_2. Yield: 0.17 g, 30%. Anal. Found: C, 45.25; H, 2.69; N, 6.14. Calcd for **3**·1.5DMF·0.75CH_2Cl_2: C, 45.35; H, 2.52; N, 6.43. IR (Nujol; cm^{-1}): 1568 ($\nu_{C=N}$). UV/vis/NIR (DMF): λ_{max}/nm (ϵ/M^{-1} cm^{-1}) 1574 (5.3 × 10^3), 995 (3.7 × 10^4), 626 (1.6 × 10^4), 523 (1.6 × 10^4), 434 (4.1 × 10^4). Electrical conductivity (S cm^{-1}): 1.5 × 10^{-5}.

X-ray Crystallography. Crystals were grown from $CHCl_3$/CH_3OH (**1b**), CH_2Cl_2/*n*-hexane (**1c**), and DMF/CH_2Cl_2 (**2** and **3**). Single-crystal X-ray diffraction measurements for **1b**, **2**·$2CH_2Cl_2$, and **3**·CH_2Cl_2·DMF were made on a Rigaku RAXIS RAPID image-plate diffractometer at 200 K and that for **1c**·CH_2Cl_2 on a Rigaku AFC5R four-cycle diffractometer using graphite-monochromated Mo Kα radiation at room temperature. Crystallographic data are summarized in Table 1. A total of 44 oscillation images for **1b** and **2**·$2CH_2Cl_2$ and a total of 74 oscillation images for **3**·CH_2Cl_2·DMF were collected. A sweep of data for **1b** and **2**·$2CH_2Cl_2$ was done using ω scans from 130.0 to 190.0° in 5.0° steps, at χ = 45.0° and ϕ = 0.0°. That for **3**·CH_2Cl_2·DMF was done using ω scans from 130.0 to 190.0° in 3.0° steps, at χ = 45.0° and ϕ = 30.0°. The exposure rate for **1b** and **3**·CH_2Cl_2·DMF was 300.0 s/deg, and that for **2**·$2CH_2Cl_2$ was 258.0 s/deg. The intensity data of **1c**·CH_2Cl_2 were collected by the ω−2θ scan mode up to 2θ = 55.0°. An empirical absorption correction was applied for each complex. The 23 871, 7555, 6648, and 10 088 independent reflections with $I > 2\sigma(I)$ of the measured 48 680, 7874, 13 532, and 20 230 reflections for **1b**, **1c**·CH_2Cl_2, **2**·$2CH_2Cl_2$, and **3**·CH_2Cl_2·DMF, respectively, were considered as "observed" and used for the structure determination. All of the structures were solved by direct methods and expanded using Fourier techniques. All non-hydrogen atoms were refined anisotropically by full-matrix least-squares methods. Hydrogen atoms for **1b** and **1c** were generated by difference Fourier synthesis and refined isotropically, while those for **2** and **3** were included in calculated positions and refined using a riding model. All calculations were performed using the *SHELXL-97* program.[16]

Results and Discussion

Synthesis, Structures, and Properties of 1a−1c. The three nickel(II) complexes **1a**−**1c** were obtained in a ratio of roughly **1a**:**1b**:**1c** = 1:3:5 from the reaction of a mixture of HL^1 and H_3L^2 with nickel(II) acetate tetrahydrate in ethanol (Scheme 2). These nickel(II) complexes were characterized by elemental analyses, UV/vis/NIR and ^{1}H NMR spectroscopies, and cyclic voltammetry, besides X-ray crystallography for **1b** and **1c**. While **1c** was also prepared by the reaction of HL^1 and nickel(II) acetate tetrahydrate, attempts to prepare **1a** upon heating **1c** in toluene, according to the previously reported procedure (Scheme 1), were unsuccessful. This indicates that the intramolecular C−C

(16) Sheldrick, G. M. *SHELXL-97. A Program for Crystal Structure Refinement*; University of Göttingen: Göttingen, Germany, 1997.

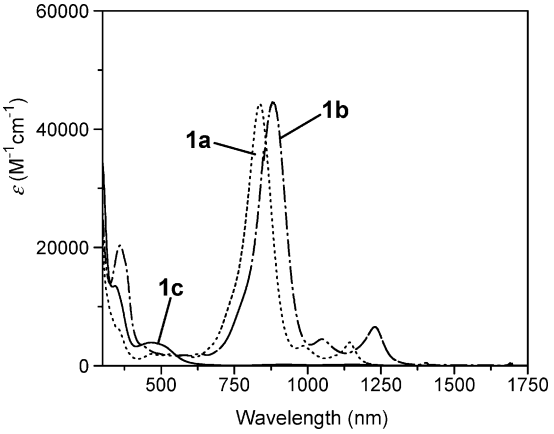

Figure 1. Absorption spectra of **1a** (dotted line), **1b** (dashed-dotted line), and **1c** (solid line) in CH_2Cl_2.

Scheme 2

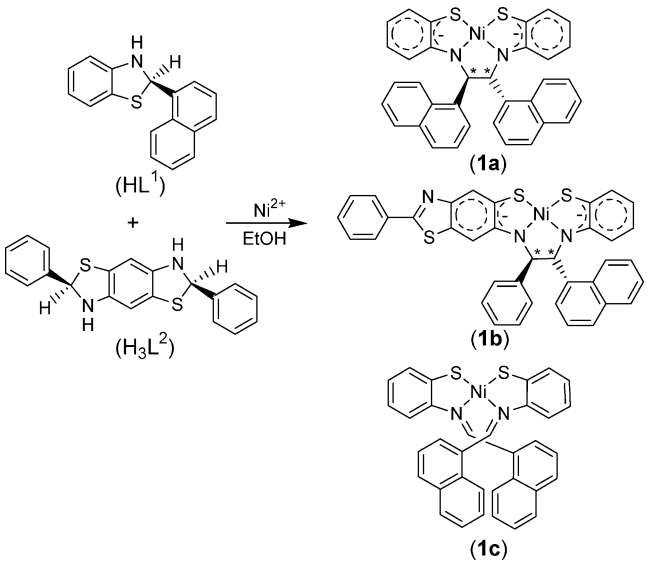

bond formation reaction in **1c** is inhibited by the steric hindrance between two 1-naphthyl groups.

The sharp N−H stretching bands found in the IR spectra of free HL^1 and H_3L^2 (3334 cm^{-1} for HL^1 and 3242 cm^{-1} for H_3L^2) were not recognized in the spectra of **1a**−**1c**, in agreement with the formation of N,S-type chelates via ring opening of benzothiazolines. The UV/vis/NIR absorption spectra of **1a**−**1c** are shown in Figure 1. Complex **1a**, which is a deep-violet color in CH_2Cl_2, gives a very intense absorption band at 837 nm ($\epsilon = 4.4 \times 10^4$ M^{-1} cm^{-1}). This absorption band is characteristic of square-planar d^8 metal complexes with non-innocent ligands,[7] including nickel(II) and platinum(II) complexes derived from 2-substituted benzothiazolines through C−C bond formation.[10] The absorption spectrum of **1b**, which is a green color in CH_2Cl_2, is similar to that of **1a** in terms of the overall shape. However, λ_{max} in the vis/NIR absorption spectrum of **1b** (885 nm and $\epsilon = 4.5 \times 10^4$ M^{-1} cm^{-1}) appears at lower energy than that of **1a**, indicative of more extensive π delocalization in **1b**. In addition, **1b** displays an intense $\pi-\pi^*$ transition based mainly on thiazole at 361 nm ($\epsilon = 2.0 \times 10^4$ M^{-1} cm^{-1}), the assignment of which is made by the comparison of its

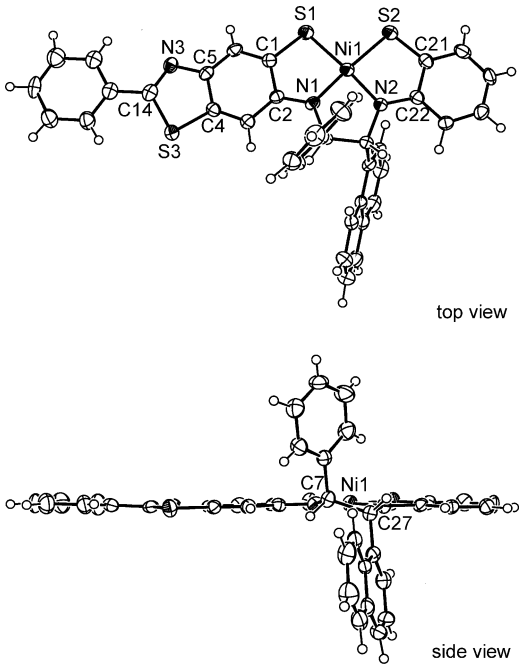

Figure 2. Molecular structure of **1b**.

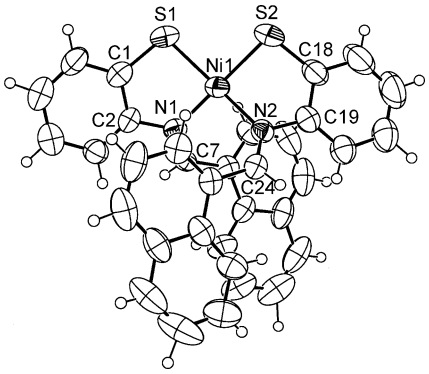

Figure 3. Molecular structure of **1c**.

absorption spectrum with that of H_3L^2.[17] On the other hand, the absorption spectrum of **1c** shows a visible band at 467 nm ($\epsilon = 3.9 \times 10^3$ M^{-1} cm^{-1}) with a shoulder on the lower energy side, and no intense absorption band is observed in the NIR region.

The ^1H NMR spectra of **1a**−**1c** are shown in Figure S1 in the Supporting Information. The ^1H NMR spectrum of **1a** shows one singlet at δ 7.15 assignable to the protons on asymmetric carbon atoms, besides six doublets and five triplets in the aromatic region. These signals correspond to a half-set of protons for **1a**. This result, along with the elemental analysis, indicates that **1a** has a symmetrical structure with a tetradentate ligand that is generated by the C−C bond formation between two bidentate-N,S ligands L^1. Of particular note for the ^1H NMR spectrum of **1b** are the characteristic four singlet resonances due to two protons on asymmetric carbon atoms (δ 7.18 and 6.32) and two protons of the N_2S_2-benzene ring (δ 8.24 and 7.65). In addition, the

(17) Roberts, M. F.; Jenekhe, S. A.; Cameron, A.; McMillan, M.; Perlstein, J. *Chem. Mater.* **1994**, *6*, 658.

Table 2. Selected Bond Distances (Å) and Angles (deg) for **1b**

Ni1−S1	2.1006(14)	N1−C7	1.486(5)
Ni1−S2	2.1229(16)	N2−C27	1.487(5)
Ni1−N1	1.801(3)	C7−C27	1.538(6)
Ni1−N2	1.806(4)	S3−C4	1.732(4)
S1−C1	1.711(4)	S3−C14	1.754(4)
S2−C21	1.702(4)	N3−C5	1.357(5)
N1−C2	1.337(5)	N3−C14	1.294(5)
N2−C22	1.335(5)		
S1−Ni1−S2	93.50(6)	S1−Ni1−N1	90.23(11)
N1−Ni1−N2	85.87(15)	S2−Ni1−N2	90.43(12)

Table 3. Selected Bond Distances (Å) and Angles (deg) for **1c**·CH_2Cl_2

Ni1−S1	2.1628(14)	N1−C2	1.421(5)
Ni1−S2	2.1650(14)	N2−C19	1.432(5)
Ni1−N1	1.916(3)	N1−C7	1.278(5)
Ni1−N2	1.936(3)	N2−C24	1.280(5)
S1−C1	1.749(5)		
S2−C18	1.744(5)		
S1−Ni1−S2	91.62(6)	S1−Ni1−N1	87.55(11)
N1−Ni1−N2	96.86(13)	S2−Ni1−N2	87.79(10)

integration and coupling patterns of the remainder of the aromatic signals confirms that **1b** has an unsymmetrical structure composed of L^1 and L^2 ligands. This result, along with the elemental analysis, suggests that **1b** contains an unsymmetrical tetradentate ligand derived from the bidentate-N,S ligands L^1 and L^2. The ^{1}H NMR spectrum of **1c** permits an easier assignment; a singlet at δ 8.19 and a doublet at δ 10.73 can be assigned to azomethine protons and ortho protons of naphthyl groups, respectively. The resonance for ortho protons of naphthyl groups in **1c** appears significantly downfield compared with those of **1a** (δ 8.30) and **1b** (δ 8.47), indicative of a strong metal−ligand interaction.[12] This result, along with the elemental analysis, indicates that **1c** has a symmetrical structure with azomethine groups. The ^{1}H NMR spectral change of **1a** was monitored as a function of time, which indicates that **1a** changes to **1c** with time in $CDCl_3$ (Figure S2 in the Supporting Information). It is seen from this result that **1a** has the same composition as **1c**, and hence **1a** and **1c** are correlated to each other as valence isomers.[10b]

The molecular structures of **1b** and **1c**, determined by single-crystal X-ray analyses, are shown in Figures 2 and 3, respectively. The selected bond distances and angles are listed in Tables 2 and 3. As shown in Figure 2, **1b** is a mononuclear nickel(II) complex having a square-planar configuration, in which a dihedral angle between the two S−Ni−N planes is 1.9°. The C−C bond (C7−C27) is formed between L^1 and L^2 to give the tetradentate ligand L^1−L^2. The L^2 moiety in **1b** contains a thiazole ring [N3−C5 = 1.357(5) Å; N3−C14 = 1.294(5) Å]. This implies that H_3L^2 is easily oxidized to thiazole, as described in a previous paper.[11] The Ni−S [2.1006(14) and 2.1229(6) Å] and Ni−N [1.806(4) and 1.801(3) Å] bond distances are shorter than the normal values of Ni−thiolato and Ni−imino distances[10] but are comparable to those reported for nickel(II) complexes with non-innocent ligands.[7,10] The C−S [1.711(4) and 1.702(4) Å] and C−N [1.337(5) and 1.335(5) Å] bond distances are typical for other non-innocent ligands.[7,10] From these results, it is obvious that **1b** has a non-innocent ligand.

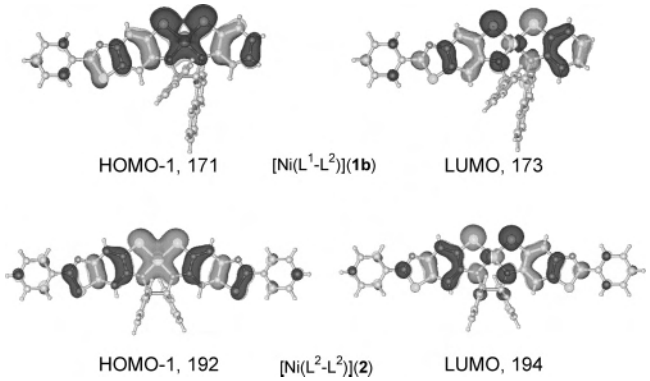

Figure 4. Molecular orbitals of **1b** and **2** based on the DV−Xα calculation.

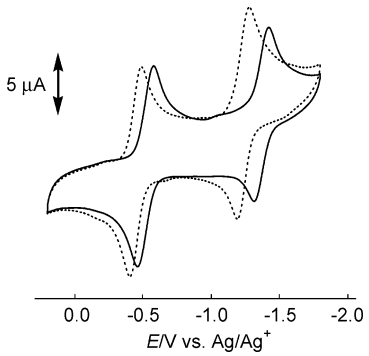

Figure 5. Cyclic voltammograms of **1a** (solid line) and **1b** (dotted line) in CH_2Cl_2 (0.10 M [(*n*-Bu)$_4$N]BF_4) with a scan rate of 0.1 V s^{-1}.

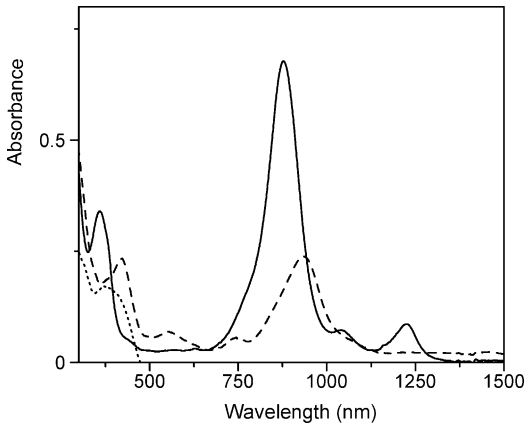

Figure 6. Absorption spectra of **1b** (solid line) and its electrochemically generated monoanion (dashed line) and dianion (dotted line) in CH_2Cl_2.

Complex **1c** consists of two bidentate-N,S ligands to form a distorted square-planar structure with a dihedral angle between the S−Ni−N planes of 21.5°. The coordination environment has a cis geometry with a N_2S_2 donor set (Figure 3). The Ni−S [2.1628(14) and 2.1650(14) Å] and Ni−N [1.916(3) and 1.936(3) Å] bond distances, which are longer than those of **1b**, are normal for four-coordinate imino-thiolato nickel(II) complexes.[10] Complex **1c** shows a molecular helicity with crossing of two pendant naphthyl groups, which is analogous to that found in [Ni(phbt)$_2$].[10]

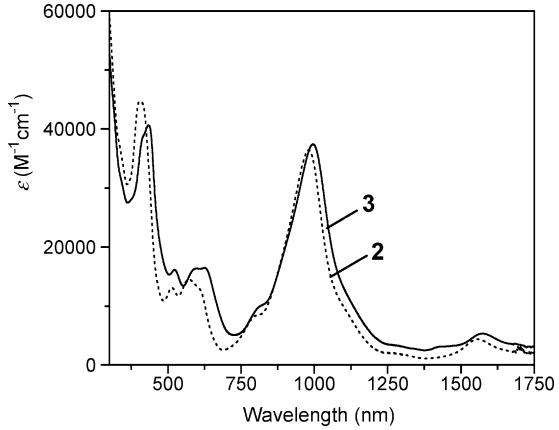

Figure 7. Absorption spectra of **2** (dotted line) and **3** (solid line) in DMF.

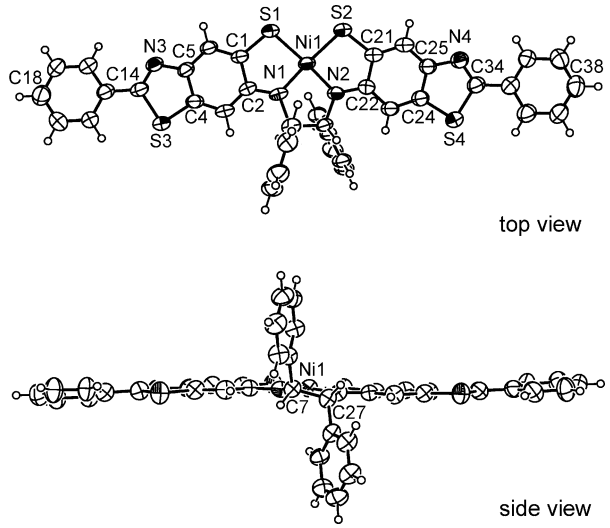

Figure 8. Molecular structure of **2**.

To gain insight into the electronic structure of **1b**, a computational study was performed by using the DV−Xα molecular orbital calculation based on the X-ray structural data. The DV−Xα calculation suggests that the intense absorption band at 885 nm is assigned to a HOMO-1(ψ_{171}) → LUMO(ψ_{173}) transition (Figure 4). This calculation also shows that not only the N_2S_2-benzene moieties but also the nickel(II) center are involved in the NIR absorption band,[18] whereas the contribution of the thiazole moiety is small and the pendant naphthyl and phenyl groups are not involved. The absorption band at 1229 nm in the NIR region is assignable as arising from the HOMO(ψ_{172}) → LUMO(ψ_{173}) transition (Figure S3 in the Supporting Information).

The electrochemistry of **1a** and **1b** was studied by cyclic voltammetry and spectroelectrochemistry. In the cyclic voltammetric studies, each complex displays two quasi-reversible reductive waves at peak potentials of $E^1_{1/2}$ = −1.368 V ($E_{pc} - E_{pa}$ = 92 mV) and $E^2_{1/2}$ = −0.524 V ($E_{pc} - E_{pa}$ = 98 mV) for **1a** and $E^1_{1/2}$ = −1.238 V ($E_{pc} - E_{pa}$ = 91 mV) and $E^2_{1/2}$ = −0.448 V ($E_{pc} - E_{pa}$ = 84 mV) for **1b** (Figure 5). The effect of the extension of conjugation in **1b** is clearly reflected in the observed redox potentials; **1b** is more easily reduced by 130 mV for $E^1_{1/2}$ and by 76 mV for $E^2_{1/2}$ than **1a**. In addition, one oxidative wave is also observed for **1a** and **1b** at $E^3_{1/2}$ = 0.780 V ($E_{pc} - E_{pa}$ = 134 mV) and $E^3_{1/2}$ = 0.756 V ($E_{pc} - E_{pa}$ = 91 mV), respectively. They are quasi-reversible and oxidative in nature.

The absorption spectra of the electrochemically generated mono- and dianions of **1b** are shown in Figure 6. While a drastic decrease in the absorbance is observed for electrochemically reduced species (**1b**$^-$ and **1b**$^{2-}$), the HOMO-1 → LUMO transition for monoanion species **1b**$^-$ is still observed in the electronic spectrum, which shifts to lower energy upon the reduction from the neutral material (885 nm for **1b** and 937 nm for **1b**$^-$). On the other hand, in the dianionic species **1b**$^{2-}$, the corresponding transition is made impossible and the absorption band does not appear in the NIR region. This behavior is similar to those of reduced forms of square-planar bis(benzene-1,2-dithiolato)metal complexes $[M(L)_2]^0$.[7e] The absorption intensity for the charge-transfer transition in the NIR region of neutral complexes with non-innocent ligands is generally weakened upon oxidation or reduction,[7] and hence it is hard to apply ionic complexes with non-innocent ligands as a favorable NIR-absorbing dye.

Synthesis, Structure, and Properties of 2. Treatment of H_3L^2 with nickel(II) acetate tetrahydrate in ethanol led to the formation of **2**. This nickel(II) complex was characterized by elemental analysis and UV/vis/NIR spectroscopy, besides X-ray crystallography. The low solubility of **2** in common solvents precluded measurements of NMR spectra and cyclic voltammograms, but UV/vis/NIR spectra could be recorded in DMF.[19]

The IR bands attributed to N−H stretching vibrations were not observed in the IR spectrum of **2**. The UV/vis/NIR absorption spectrum of **2** gives an intense absorption band at 981 nm (Figure 7), which is fairly red-shifted compared with those of **1a** and **1b** with a slight reduction in ϵ_{max} (3.6×10^4 M^{-1} cm^{-1} for **2**, 4.4×10^4 M^{-1} cm^{-1} for **1a**, and 4.5×10^4 M^{-1} cm^{-1} for **1b**). This is in agreement with the extension of π conjugation in **2**. In addition, the presence of

Table 4. Selected Bond Distances (Å) and Angles (deg) for **2**·2CH_2Cl_2

Ni1−S1	2.112(2)	N1−C7	1.464(5)
Ni1−S2	2.1129(18)	N2−C27	1.469(5)
Ni1−N1	1.802(4)	C7−C27	1.536(6)
Ni1−N2	1.798(4)	S3−C4	1.719(5)
S1−C1	1.723(5)	S3−C14	1.743(5)
S2−C21	1.716(5)	N3−C5	1.363(6)
N1−C2	1.350(6)	N3−C14	1.274(6)
N2−C22	1.354(6)	S4−C24	1.721(5)
		S4−C34	1.756(5)
		N4−C25	1.380(6)
		N4−C34	1.283(6)
S1−Ni1−S2	95.11(7)	S1−Ni1−N1	88.97(13)
N1−Ni1−N2	86.72(17)	S2−Ni1−N2	89.19(13)

(18) In a preliminary experiment, the characteristic NIR absorption band in the cobalt(II) complex, [Co(L^1−L^2)], showed a pronounced blue shift (705 nm) compared with that of the corresponding nickel(II) complex (**1b**).

(19) The absorption spectra of **1a** and **1b** in DMF display intense bands at 833 and 887 nm, respectively.

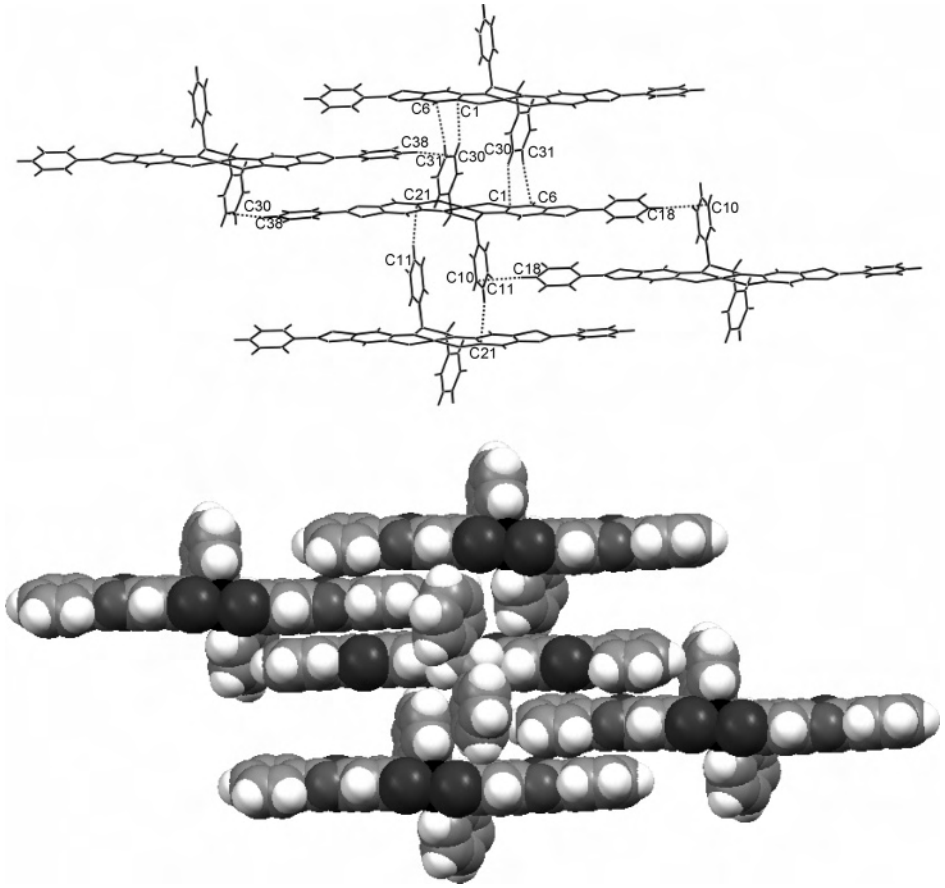

Figure 9. Crystal structure of **2** showing intermolecular contacts (top) and its space-filling form showing the stacking perpendicular to the molecular planes (bottom).

Scheme 3

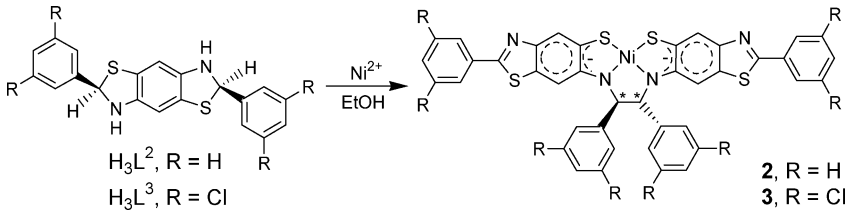

two thiazole moieties in **2** is reflected in the intensity of the absorption band at 404 nm ($\epsilon = 4.5 \times 10^4\ M^{-1}\ cm^{-1}$), which is about 2 times that of **1b** ($\epsilon = 2.0 \times 10^4\ M^{-1}\ cm^{-1}$) having one thiazole moiety.

From DV−Xα calculation based on the X-ray structural data of **2** (vide infra), the absorption band at 981 nm is assigned to a HOMO-1(ψ_{192}) → LUMO(ψ_{194}) transition (Figure 4). This calculation also indicates that the extended π system containing a thiazole ring of **2** is profoundly involved in the NIR absorption band. The absorption band for the HOMO(ψ_{193}) → LUMO(ψ_{194}) transition is observed at 1559 nm (Figure S3 in the Supporting Information).

The molecular structure of **2** is shown in Figure 8, and the selected bond distances and angles are listed in Table 4. Complex **2** consists of a tetradentate ligand, which was generated by C−C bond formation (C7−C27) between the two L^2 ligands, accompanied by partial oxidation to form thiazole rings. The geometry around the nickel(II) center is square-planar with a dihedral angle between the S−Ni−N planes of 0.8°. The Ni−S [2.112(2) and 2.1129(18) Å] and Ni−N [1.802(4) and 1.798(4) Å] bond distances are typical values found for other complexes with non-innocent ligands and so are the C−S [1.723(5) and 1.716(5) Å] and C−N [1.350(6) and 1.354(6) Å] bond distances.[7,10] Thus, **2** is regarded as a complex with a non-innocent ligand, which has extended coplanar planes, with the two terminal carbon atoms (C18 and C38) being separated by 22.883(9) Å. The packing structure of **2** is shown in Figure 9. Each molecule is surrounded by four neighboring molecules to form a 2-D sheet structure interpenetrated to each other, aided by eight edge-to-face interactions between the pendant phenyl groups and the basal planes of molecules [C−C contacts (Å): C1···C30 = 3.533(7), C6···C31 = 3.518(7), C10···C18 = 3.732(8), C11···C21 = 3.573(7), C30···C38 = 3.67(1)]. The interplanar angles between benzene rings showing short contacts are 92.5−96.8°. The shortest Ni···Ni distance is 8.1394(8) Å.

Table 5. Selected Bond Distances (Å) and Angles (deg) for $3 \cdot CH_2Cl_2 \cdot DMF$

Ni1−S1	2.126(10)	N1−C7	1.464(11)
Ni1−S2	2.132(5)	N2−C27	1.467(10)
Ni1−N1	1.815(7)	C7−C27	1.515(12)
Ni1−N2	1.818(10)	S3−C4	1.727(9)
S1−C1	1.712(9)	S3−C14	1.748(12)
S2−C21	1.711(11)	N3−C5	1.389(11)
N1−C2	1.339(11)	N3−C14	1.295(10)
N2−C22	1.353(10)	S4−C24	1.710(11)
		S4−C34	1.763(9)
		N4−C25	1.379(10)
		N4−C34	1.279(11)
S1−Ni1−S2	94.9(3)	S1−Ni1−N1	89.7(3)
N1−Ni1−N2	85.6(4)	S2−Ni1−N2	89.7(3)

As mentioned above, there are CH/π interactions between the protons of pendant phenyl groups and the N_2S_2-benzene moieties of neighboring molecules in the crystal structure of **2**. It is expected that such intermolecular interactions produce conduction paths to induce appreciable conductivity. However, a room-temperature electrical conductivity of **2** in a compressed powder pellet was only 5.9×10^{-8} S cm^{-1}. Thus, in the solid phase of **2**, the intermolecular contact due to CH/π interactions seems to be inadequate to form effective electron conduction pathways.

Synthesis, Structure, and Properties of 3. To improve the electrical conductivity of **2**, we employed H_3L^3 as a starting material, which is expected to form a packing structure different from that of **2** by replacing the hydrogen atoms of the pendant phenyl rings in H_3L^2 with chlorine atoms (Scheme 3). This starting reagent H_3L^3 was synthesized according to the procedures for H_3L^2 and characterized by elemental analysis and IR and ^{1}H NMR spectroscopies.[11] Treatment of H_3L^3 with nickel(II) acetate tetrahydrate in ethanol led to the formation of **3**. This nickel(II) complex was characterized by elemental analysis and UV/vis/NIR spectroscopy, besides X-ray crystallography.

The UV/vis/NIR absorption spectrum of **3** (Figure 7) gives an intense NIR band at 995 nm ($\epsilon = 3.7 \times 10^4$ M^{-1} cm^{-1}), besides an intense visible band at 434 nm ($\epsilon = 4.1 \times 10^4$ M^{-1} cm^{-1}). The NIR absorption band of **3** is slightly red-shifted compared with that of **2**. In addition, diffuse-reflectance spectra of **2** and **3** reveal two broad bands at 990 and 1324 nm and at 1004 and 1358 nm, respectively (Figure S4 in the Supporting Information).

From the DV−Xα calculation on **3**, it is suggested that the absorption bands at 995 and 1574 nm are assigned to HOMO-1(ψ_{256}) → LUMO(ψ_{258}) and HOMO(ψ_{257}) → LUMO(ψ_{258}) transitions, respectively (Figure S5 in the Supporting Information). This result indicates that the extended π system composed of the N_2S_2-benzene and thiazole moieties containing the nickel(II) center exerts a great influence on NIR absorption.

The structure of **3** was also determined by single-crystal X-ray analysis. The selected bond distances and angles are listed in Table 5. As shown in Figure 10, **3** has a square-planar configuration as **2** does. The dihedral angle between the S−Ni−N planes is 2.9°. The tetradentate-N_2S_2 ligand is formed through C−C bond formation (C7−C27) between

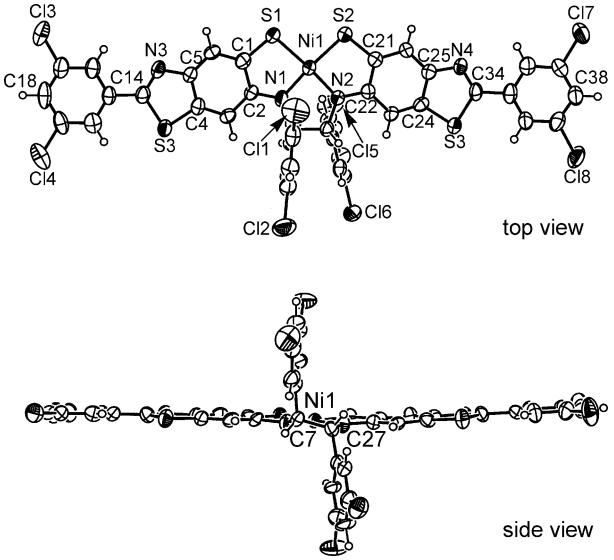

Figure 10. Molecular structure of **3**.

the two partly oxidized L^3 ligands. A consideration of the Ni−S [2.126(10) and 2.132(5) Å], Ni−N [1.815(7) and 1.818(10) Å], C−S [1.712(9) and 1.711(11) Å], and C−N [1.339(11) and 1.353(10) Å] bond distances, which are similar to those observed in complexes with non-innocent ligands,[7,10] supports that **3**, as well as **2**, is a complex with a non-innocent ligand. The π-conjugated system of **3** is as large as that of **2** with the C18···C38 distance of 22.92(2) Å. The packing structure of **3** is shown in Figure 11. In **3**, each molecule is surrounded by five neighboring molecules to form a 2-D sheet structure, stacked perpendicularly to the molecular plane. The crystallization solvents are among the 2-D sheets, and no transverse interaction between the 2-D sheets is found. The shortest Ni···Ni distance is 7.150(2) Å. The most interesting feature of the crystal structure in **3** is that there exist face-to-face interactions [C−S contact (Å), S1···C5 = 3.454(8); C−C contacts, C1···C1 = 3.40(1), C26···C39 = 3.39(1) Å], which are not observed in **2**, besides three edge-to-face interactions between the pendant phenyl groups and the basal planes of complexes [C10···C18 = 3.76(2) Å, C11···C35 = 3.69(1) Å, and C11···C36 = 3.55(1) Å]. The corresponding interplanar angles in the face-to-face and edge-to-face interactions are 0.0−1.4° and 87.7−96.3°, respectively. In addition, two weak CH···N hydrogen bonds are observed between the pendant phenyl groups and the thiazole rings of the basal planes [C29···N3 = 3.40(1) Å; C−H···N = 157.1°].[20] Although **3** has chlorine atoms in the pendant phenyl ring and thus is expected to be more sterically crowded compared with **2**, the molecule of **3** aggregates in a more compact manner (D_{calcd} = 1.537 g cm^{-3} for **2** and 1.635 g cm^{-3} for **3**) via several intermolecular interactions containing face-to-face interactions as depicted in Figure 11.

(20) (a) Alekseyeva, E. S.; Batsanov, A. S.; Boyd, L. A.; Fox, M. A.; Hibbert, T. G.; Howard, J. A. K.; MacBride, J. A. H.; Mackinnon, A.; Wade, K. *Dalton Trans.* **2003**, 475. (b) Cappelli, A.; Giorgi, G.; Anzini, M.; Vomero, S.; Ristori, S.; Rossi, C.; Donati, A. *Chem.—Eur. J.* **2004**, *10*, 3177.

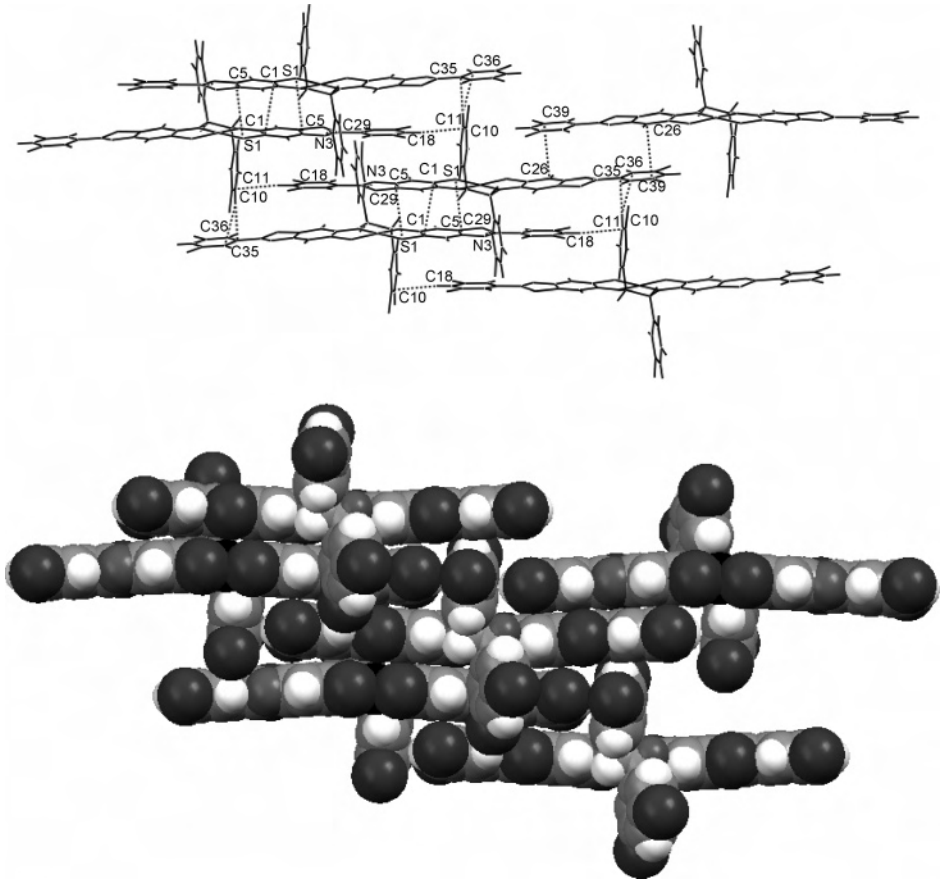

Figure 11. Crystal structure of **3** showing intermolecular contacts (top) and its space-filling form showing the stacking perpendicular to the molecular planes (bottom).

A pressed pellet of powdered **3** displays a room-temperature electrical conductivity of 1.5×10^{-5} S cm^{-1}. This conductivity, while not especially high relative to those for the reported single-component molecular conductors,[3−5,21] is noteworthy for the solid sample that has neither S···S contacts nor M···M interactions.[3] The electrical conductivity of **3** is presumably due to the presence of partially filled HOMO and LUMO bands, which is introduced by the large intermolecular overlap and the small HOMO–LUMO energy gap owing to an extended π-conjugated system, as indicated by the reflectance spectrum. Judging from the electrical conductivities (1.5×10^{-5} S cm^{-1} for **3** and 5.9×10^{-8} S cm^{-1} for **2**), it may be considered that the molecular array with face-to-face interactions, which can form a dense stacking structure, is more suitable for the construction of electron-conduction pathways than that with edge-to-face interactions.

Conclusion

The three kinds of nickel(II) complexes, [Ni(L^1−L^1)] (**1a**), [Ni(L^1−L^2)] (**1b**), and [Ni(L^1)$_2$] (**1c**), were prepared by treating nickel(II) acetate with a mixture of HL^1 and H_3L^2. Treatment of nickel(II) acetate with H_3L^2 afforded [Ni(L^2−L^2)] (**2**) having a π-conjugated system. Complex **2** exhibits a very intense absorption band at lower energy than those of **1a** and **1b**, reflecting the more extended conjugate system. The corresponding reaction with H_3L^3 gave [Ni(L^3−L^3)] (**3**), which shows a very intense absorption band at the lowest energy for the nickel(II) complexes with non-innocent ligands in the present work. These results indicate that the fine control of the NIR absorption is possible through the adjustment of π-conjugated systems. Note that **3** shows an electrical conductivity of 1.5×10^{-5} S cm^{-1}, which is significantly higher than that of **2** (5.9×10^{-8} S cm^{-1}). This behavior may be correlated to the difference in packing structures, in which edge-to-face and face-to-face intermolecular interactions are mainly observed for **2** and **3**, respectively. Finally, the present results indicate that multifunctional nickel(II) complexes available as both NIR-absorbing dyes and semiconductors could be prepared through the subtle changes of the π-conjugated ligands. Further studies to construct 3-D assemblies with transverse interactions are in progress in our laboratory.

Acknowledgment. We gratefully thank Dr. Motohiro Nakano for the electrical resistivity measurements.

Supporting Information Available: Figures S1−S5 and X-ray crystallographic files in CIF format for the structures in this work. This material is available free of charge via the Internet at http://pubs.acs.org.

IC0618246

(21) (a) Belo, D.; Alves, H.; Lopes, E. B.; Duarte, M. T.; Gama, V.; Henriques, R. T.; Almeida, M.; Pérez-Benítez, A.; Rovira, C.; Veciana, J. A. *Chem.—Eur. J.* **2001**, *7*, 511. (b) Itkis, M. E.; Chi, X.; Cordes, A. W.; Haddon, R. C. *Science* **2002**, *296*, 1443.